Hindawi
Mathematical Problems in Engineering
Volume 2018, Article ID 5631714, 10 pages
https://doi.org/10.1155/2018/5631714

Research Article

Joint DOA and Polarization Estimation with Two Parallel Sparse Dipole Arrays

Jian Xie[1,2] **Ling Wang**[1,2] **and Zhaolin Zhang**[2]

[1]*Research & Development Institute of Northwestern Polytechnical University in Shenzhen, Shenzhen 518057, China*
[2]*Electronics and Information School, Northwestern Polytechnical University, Xi'an 710072, China*

Correspondence should be addressed to Jian Xie; xiejian@nwpu.edu.cn

Received 7 August 2018; Revised 15 December 2018; Accepted 18 December 2018; Published 31 December 2018

Academic Editor: Volodymyr Ponomaryov

Electromagnetic vector sensors (EMVS) have attracted growing attention in recent years. However, the mutual coupling effects in practical EMVS arrays may seriously degrade the parameter estimation performance. In order to solve this problem, a novel array configuration consisting of two parallel sparse dipole arrays is proposed. Based on the spatially rotational invariance property between the two parallel arrays and the interdipole spacing inside each array, highly accurate but ambiguous direction-cosine estimates, coarse direction-of-arrival (DOA) estimates, and polarization parameter estimation can be obtained jointly. The coarse DOA estimates are then employed to disambiguate the phase ambiguities in the fine estimates. Compared with collocated EMVS, the proposed array overcomes the mutual coupling problem. Moreover, the DOA estimation accuracy is promoted due to the sparse array aperture extension. Simulation results demonstrate the effectiveness of the proposed algorithm.

1. Introduction

Source localization and polarization estimation using electromagnetic vector sensors (EMVS) have received considerable attention over the past decades. Generally, an electromagnetic vector sensor consists of three orthogonal electrically short dipoles and three orthogonal magnetically small loops [1–4]. All of the six components are spatially collocated in a point-like geometry, and no spatial phase-factor exists among them. Many advanced algorithms have been developed for direction finding, polarization estimation, and tracking schemes [5–9]. Particularly, a lot of eigenstructure-based direction finding and polarization estimation schemes have been presented in recent years. In [10], a temporal-invariance version estimation of signal parameters via rotational invariance technique (ESPRIT) [11] has been applied for a single collocated six-component vector sensor to estimate the arrival angles and polarization states of multiple pure tones. In [12], a spatial-invariance version of ESPRIT has been used for some collocated EVMS's deployed in a sparse rectangular grid without incurring cyclic ambiguity in the final estimates of the sources' direction parameters. In [13, 14], a spatial-invariance version of ESPRIT has been proposed for arbitrarily spaced EVMS's, whose locations are unknown. In [15], based on a spatially collocated EMVS, the author uses vector cross-product to perform direction finding for multiple noncooperative wideband fast frequency-hop signals.

In the above-mentioned literature, the algorithms mostly presume that all the six components of EMVS are utilized. However, the responses of electric field and magnetic field may be different between each other in practical systems. Therefore, in [16] Wong proposed to deploy only one triad to mitigate this problem. In [17], the authors utilized a triad of collocated and perpendicular electrically short dipoles (or of electrically small loops) and derived the Cramér-Rao lower bound accounting for the possibility of failure in any individual dipoles (or loops). Recently, aiming at the low radiation efficiency of such short dipoles or small loops, the authors developed a triad of electrically large circular loops for the estimation of an incident emitter's direction-of-arrival (DOA) or polarization [18]. Similarly, in [19], the authors proposed a triad of electrically "long" dipoles for direction finding and polarization estimation. However, both of them adopted a spatially collocated array structure. Therefore, the

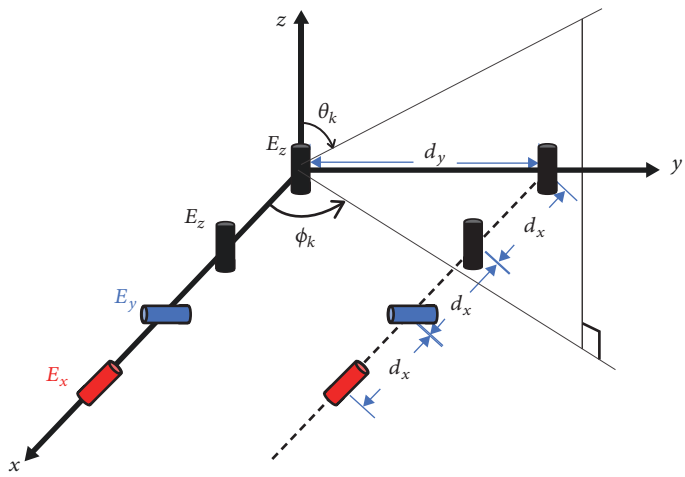

Figure 1: Two parallel spatially spread dipole arrays configuration.

mutual coupling effect of these collocated triad structure is strong, and the developed algorithms require the prior knowledge of polarization information, which is often invalid in practical applications.

Note that the mutual coupling effect across the collocated dipoles/loops is neglected in the above-mentioned literature. However, the mutual coupling may degrade the parameters estimation performance and increase the hardware cost of the vector sensors. Therefore, a vector cross-product direction finding algorithm is proposed in [20, 21] for six orthogonally oriented but spatially noncollocating dipoles/loops. However, the algorithm developed there requires a temporal invariance of the incident sources, which is often invalid in practical. Moreover, the array structure proposed is spatially displaced along one direction; thus it cannot only provide high accuracy and unambiguous DOA estimates. In [22], the author developed a sparse array composed of three noncollocating dipole (or loop) triads. Based on the ESPRIT principle, the high accuracy and unambiguous estimates of DOA and polarization parameters are obtained. However, the direction-cosines estimates along x and y axes are obtained from two independent eigendecomposition operations; thus they require additional parameter matching procedure. In [23], the author advanced spatially spread dipole/loop quads/quints for direction finding and polarization estimation. However, it assumes that the source signals are pure tones which may be invalid in practical scenarios. In [24], the authors proposed a spatially spread quint of only dipoles or loops, for DOA and polarization estimation. Based on the centrosymmetric array, the authors develop a DOA and polarization estimator via vector-cross-product. However, it requires a 2D search process for conducting coarse 2D-DOA estimation, which is computationally inefficient. In [25–27], the authors utilize different types of spatially separated dipoles/loops to constructs a sparse planar array. This kind of structure can provide high accuracy DOA estimates of multiple sources. However, the direction-cosines estimates along x and y axes are obtained from two independent eigendecomposition operations; thus they require additional parameter matching procedure.

Aiming at addressing the above-mentioned problems, we propose in this paper a novel array configuration which consists of two parallel sparse dipole arrays. Based on the spatially rotational invariance property between the two parallel arrays and the interdipole spacing inside each array, highly accurate but ambiguous direction-cosine estimates, coarse DOA estimates, and polarization parameters estimation can be obtained jointly. The coarse DOA estimates are then employed to yield the final DOA estimates with high accuracy.

Compared with the traditional methods, the proposed scheme enjoys the following advantages: (1) The interdipole spacing and intersubarray spacing can be extended much greater than half a wavelength, which could reduce the mutual coupling effect. (2) High accuracy 2D DOA estimates can be obtained for the azimuth angle and the elevation angle concurrently, due to the extended aperture in both directions. (3) Only dipoles are utilized in the array, which avoids the responses mismatch of dipoles and loops. (4) The parameters are derived in closed-form and are therefore computationally efficient. (5) The DOA and polarization parameters are paired automatically. (6) The source signals are not required to be pure tones.

The rest of the paper is organized as follows: Section 2 introduces the signal model of the parallel spatially spread dipole arrays. The proposed algorithm is described in Section 3. In Section 4, simulations are conducted to validate the performance of our method. We conclude this paper in Section 5.

Throughout the paper, the complex conjugate, transpose, Hermitian transpose, and pseudoinverse are denoted by $(\bullet)^*$, $(\bullet)^T$, $(\bullet)^H$, and $(\bullet)^\dagger$, respectively. $\mathbf{I}_m$ represents a $m\times m$ identity matrix, and $\mathbf{O}_m$ is a $m\times m$ zero matrix.

2. Signal Model

In order to obtain high accuracy elevation and azimuth DOA estimates, we construct an array composed of two parallel dipole arrays as shown in Figure 1. Note that each

dipole array consists of four dipoles that are uniformly spread along the x-axis, with the interelements spacing being d_x. At the origin of a Cartesian coordinate system, a short dipole antenna element denoted as E_z is placed along the z-axis. The other three of the dipoles (denoted as E_x, E_y, and E_z) are orthogonally oriented along each of the x-axis, y-axis, and z-axis. In addition, the displacement along the y-axis between the two parallel arrays is d_y.

It is well known that, for a completely polarized unit power transverse electromagnetic wave travelling through a homogeneous isotropic medium, it can be characterized by a 3×1 electric-field vector in the Cartesian coordinate system [1]:

$$\begin{aligned}\mathbf{e}(\theta,\phi,\gamma,\eta) &= \begin{bmatrix} e_x \\ e_y \\ e_z \end{bmatrix} \\ &= \begin{bmatrix} \cos\theta\cos\phi & -\sin\phi \\ \cos\theta\sin\phi & \cos\phi \\ -\sin\theta & 0 \end{bmatrix} \begin{bmatrix} \sin\gamma e^{j\eta} \\ \cos\gamma \end{bmatrix}\end{aligned} \tag{1}$$

where $\theta \in [0,\pi]$ is the signal's elevation angle measured from the positive z-axis, $\phi \in [0,2\pi)$ denotes the azimuth angle measured from the positive x-axis, $\gamma \in [0,\pi/2)$ stands for the auxiliary polarization angle, and $\eta \in [-\pi,\pi)$ refers to the polarization phase difference.

Considering the spatial phase shift introduced by displacement along the x-axis, the array manifold of the four spatially spread dipoles on the left-hand side can be expressed as

$$\mathbf{a}(\theta,\phi,\gamma,\eta) = \begin{bmatrix} e_x \\ e_y \\ e_z \\ e_z \end{bmatrix} \odot \begin{bmatrix} e^{-j(2\pi/\lambda)3d_x u} \\ e^{-j(2\pi/\lambda)2d_x u} \\ e^{-j(2\pi/\lambda)d_x u} \\ 1 \end{bmatrix} \tag{2}$$

Herein, $\odot$ denotes the Hadamard product, and $u = \sin\theta\cos\phi$ represents the direction-cosine of the x-axis. Note that the interdipole displacement along the x-axis could be utilized to extend the array aperture and also reduce the mutual coupling.

To obtain the aperture expansion along the y-axis, another dipole-quad array with the same structure is added in parallel, and the displacement along the y-axis d_y can be much greater than a half wavelength. Considering the spatial phase-factor introduced by the parallel array structure, the array manifold can be expressed as

$$\mathbf{b}(\theta,\phi,\gamma,\eta) = \begin{bmatrix} \mathbf{a} \\ \mathbf{a}\cdot e^{-j(2\pi/\lambda)d_y v} \end{bmatrix} \tag{3}$$

and $v = \sin\theta\sin\phi$ represents the direction-cosine of the y-axis.

Assume that there are a total of K signals impinging onto the proposed array from the far-field. Thus, the received signal data can be expressed as follows:

$$\mathbf{x}(t) = \sum_{k=1}^{K} \mathbf{b}_k s_k(t) + \mathbf{n}(t) = \mathbf{B}\mathbf{s}(t) + \mathbf{n}(t) \tag{4}$$

$$\mathbf{B} = \left[\mathbf{b}(\theta_1,\phi_1,\gamma_1,\eta_1),\cdots,\mathbf{b}(\theta_K,\phi_K,\gamma_K,\eta_K)\right] \tag{5}$$

$$\mathbf{s}(t) = \left[s_1(t),\cdots,s_K(t)\right]^T \tag{6}$$

where $\mathbf{B}$ is the array manifold, $\mathbf{s}(t)$ is the signal vector, and $\mathbf{n}(t)$ denotes the additive Gaussian white noise.

Given a total number of L snapshots generated at the distinct instants $\{t_l: l = 1,...,L\}$, the main problem to be addressed in this paper is to obtain high accuracy 2D DOA estimates from these snapshots, i.e., estimate the azimuth angle and elevation angle parameters $\{\theta_k,\phi_k\}$, $k = 1,\cdots,K$ of the impinging signals. Moreover, for beamforming purposes, it may be also useful to estimate the corresponding polarization parameters $\{\gamma_k,\eta_k\}$, $k = 1,\cdots,K$.

Unlike the traditional scalar array antenna model, the proposed parallel sparse dipole arrays in Figure 1 are polarized, sparsely spread, and composed of noncollocating orthogonally oriented dipoles. Therefore, a novel algorithm is investigated in the next section for the polarized antenna arrays.

3. Proposed Algorithm

In order to generate unambiguous 2D DOA and polarization parameters with high accuracy for the proposed polarized array, our algorithm creatively uses the ESPRIT technique through the following stages: (1) based on the spatial rotational invariance property between the two parallel arrays, ESPRIT is utilized to generate the eigenvalues and the eigenvectors; (2) the eigenvalues offer the estimates of high accuracy but ambiguous y-axis direction-cosines; (3) the relationships between the elements of each source's steering vector $\mathbf{a}(\theta,\phi,\gamma,\eta)$ are employed to obtain ambiguous high accuracy but ambiguous x-axis direction-cosine estimates, coarse 2D DOA estimates, and polarization parameter estimation; (4) the coarse DOA estimation results are employed to select a set of highly accurate and unambiguous direction-cosine estimates from the set containing the cyclically ambiguous estimates.

3.1. High Accuracy and Cyclically Ambiguous y-Axis Direction-Cosine Estimation. It can be seen from (3) that the first and the last four components of the steering vector $\mathbf{b}_k$ satisfy the spatial rotational invariance, which corresponds to the two parallel dipole arrays, respectively. For the kth source, this rotational invariance property can be expressed as

$$\mathbf{J}_2\mathbf{b}_k = \mathbf{J}_1\mathbf{b}_k e^{-j(2\pi/\lambda)d_y v_k}, \quad k = 1,\cdots,K \tag{7}$$

$$\begin{aligned}\mathbf{J}_1 &= \left[\mathbf{I}_4 \;\; \mathbf{O}_4\right], \\ \mathbf{J}_2 &= \left[\mathbf{O}_4 \;\; \mathbf{I}_4\right]\end{aligned} \tag{8}$$

where $\mathbf{J}_1$ and $\mathbf{J}_2$ are the selection matrices.

Considering the K far-field radiating sources received by the array, the spatial rotational invariance property can be generalized as the following matrix form:

$$\mathbf{J}_2\mathbf{B} = \mathbf{J}_1\mathbf{B}\boldsymbol{\Phi}_v \tag{9}$$

$$\boldsymbol{\Phi}_v = \operatorname{diag}\left[\exp\left(-j\frac{2\pi}{\lambda}d_y v_1\right), \exp\left(-j\frac{2\pi}{\lambda}d_y v_2\right), \cdots, \exp\left(-j\frac{2\pi}{\lambda}d_y v_K\right)\right] \tag{10}$$

where diag[$\mathbf{v}$] represents a diagonal matrix with its main diagonal elements being those of $\mathbf{v}$.

It is noticeable that $\boldsymbol{\Phi}_v$ contains the y-axis direction-cosine information. Therefore, to obtain the estimation of $\boldsymbol{\Phi}_v$, we first generate the covariance matrix of the received data $\mathbf{x}(t)$:

$$\mathbf{R}_X = E\left\{\mathbf{x}(t)\,\mathbf{x}^H(t)\right\} = \mathbf{B}\mathbf{R}_s\mathbf{B}^H + \sigma_n^2\mathbf{I} \tag{11}$$

where $E\{\bullet\}$ denotes expectation. By taking the eigenvalue decomposition (EVD) of $\mathbf{R}_X$, we have the following equation:

$$\mathbf{R}_X = \mathbf{E}_S\boldsymbol{\Lambda}_S\mathbf{E}_S^H + \mathbf{E}_N\boldsymbol{\Lambda}_N\mathbf{E}_N^H \tag{12}$$

where $\boldsymbol{\Lambda}_S$ is a diagonal matrix containing K largest eigenvalues and $\boldsymbol{\Lambda}_N$ is a diagonal matrix associated with the remaining 8-K ones. $\mathbf{E}_S$, which spans the signal subspace of $\mathbf{R}_X$, is composed of the K vectors corresponding to the K largest eigenvalues of $\mathbf{R}_X$. $\mathbf{E}_N$, which spans the noise subspace of $\mathbf{R}_X$, is composed of the remaining 8-K vectors corresponding to the 8-K small eigenvalues of $\mathbf{R}_X$.

Based on the subspace principle, the 8×K signal subspace matrix can be expressed as

$$\mathbf{E}_S = \mathbf{B}\mathbf{T} \tag{13}$$

where $\mathbf{T}$ denotes an unknown K×K nonsingular matrix to be determined. Therefore, according to (9) and (13), the following relationships can be derived:

$$\mathbf{E}_{S1} = \mathbf{J}_1\mathbf{E}_S = \mathbf{J}_1\mathbf{B}\mathbf{T} \tag{14}$$

$$\mathbf{E}_{S2} = \mathbf{J}_2\mathbf{E}_S = \mathbf{J}_2\mathbf{B}\mathbf{T} = \mathbf{J}_1\mathbf{B}\boldsymbol{\Phi}_v\mathbf{T} = \mathbf{E}_{S1}\boldsymbol{\Phi}_v \tag{15}$$

Applying the least squares (LS) algorithm [11], we have

$$\mathbf{E}_{S1}^{\dagger}\mathbf{E}_{S2} = \mathbf{T}^{-1}\boldsymbol{\Phi}_v\mathbf{T} \tag{16}$$

where $(\bullet)^{\dagger}$ denotes the Moore-Penrose inverse. The eigenvalue decomposition of the matrix $\mathbf{E}_{S1}^{\dagger}\mathbf{E}_{S2}$ yields the estimates of $\mathbf{T}$ and $\boldsymbol{\Phi}_v$, respectively. And the main diagonal elements of $\boldsymbol{\Phi}_v$ are composed of the eigenvalues of $\mathbf{E}_{S1}^{\dagger}\mathbf{E}_{S2}$. Therefore, the direction-cosine along the y-axis can be obtained by

$$v_k^{fine} = -\frac{\angle\left[\boldsymbol{\Phi}_v\right]_{k,k}}{2\pi d_y/\lambda}, \quad k = 1, \cdots, K \tag{17}$$

where the $\angle(\bullet)$ operator returns the phase of the complex number in its argument.

Note that when the displacement parameter d_y between the two parallel dipole arrays is much greater than half a wavelength, these direction-cosines estimation values in (17) will be of high accuracy, due to the extend aperture size along the y-axis. However, they will suffer from cyclical ambiguity problem at the same time.

3.2. High Accuracy and Cyclically Ambiguous x-Axis Direction-Cosine Estimation. Since the nonsingular matrix $\mathbf{T}$ has been determined in the above subsection, the manifold matrix of the left-hand side subarray can be estimated from the following expression:

$$\left[\widehat{\mathbf{a}}_1, \widehat{\mathbf{a}}_2, \cdots, \widehat{\mathbf{a}}_K\right] = \frac{1}{2}c\left\{\mathbf{J}_1\widehat{\mathbf{E}}_S\widehat{\mathbf{T}}^{-1} + \mathbf{J}_2\widehat{\mathbf{E}}_S\widehat{\mathbf{T}}^{-1}\widehat{\boldsymbol{\Phi}}_v^{-1}\right\} \tag{18}$$

where $\widehat{\mathbf{a}}_k$ represents the estimation of $\mathbf{a}(\theta_k, \phi_k, \gamma_k, \eta_k)$ and c is an unknown complex constant.

According to the array structure in Figure 1 and (2), the array manifold of the left-hand side subarray can be estimated as

$$\widehat{\mathbf{a}}_k = c\mathbf{a} = c\begin{bmatrix} \left(\sin\gamma_k\cos\theta_k\cos\phi_k e^{j\eta_k} - \cos\gamma_k\sin\phi_k\right)e^{-j(2\pi/\lambda)3d_x u} \\ \left(\sin\gamma_k\cos\theta_k\sin\phi_k e^{j\eta_k} + \cos\gamma_k\cos\phi_k\right)e^{-j(2\pi/\lambda)2d_x u} \\ \left(-\sin\gamma_k\sin\theta_k e^{j\eta_k}\right)e^{-j(2\pi/\lambda)d_x u} \\ -\sin\gamma_k\sin\theta_k e^{j\eta_k} \end{bmatrix} \tag{19}$$

Based on the estimated steering vector $\widehat{\mathbf{a}}_k$, the direction-cosine of x-axis can be calculated

$$u_k^{fine} = \frac{\angle\left\{\left[\widehat{\mathbf{a}}_k\right]_4 / \left[\widehat{\mathbf{a}}_k\right]_3\right\}}{2\pi d_x/\lambda} \tag{20}$$

where the $\angle\{\bullet\}$ operator returns the phase of the complex number in its argument and $[\widehat{\mathbf{a}}]_i$ denotes the ith entry of $\widehat{\mathbf{a}}$.

Similarly, when the interdipole spacing parameter d_x is much greater than half a wavelength, these direction-cosines estimation values in (20) will be of high accuracy, due to the extend aperture size along the x-axis. However, they will suffer from cyclical ambiguity problem at the same time.

3.3. Coarse and Unambiguous 2D-DOA Estimation. With the estimation of the steering vector $\widehat{\mathbf{a}}_k$, we can construct the following 2×1 vector

$$\begin{aligned} \mathbf{q}_k &= \begin{bmatrix} \dfrac{\left[\widehat{\mathbf{a}}_k\right]_1}{\left[\widehat{\mathbf{a}}_k\right]_3}\cdot e^{j2\angle\{[\widehat{\mathbf{a}}_k]_4/[\widehat{\mathbf{a}}_k]_3\}} \\ \dfrac{\left[\widehat{\mathbf{a}}_k\right]_2}{\left[\widehat{\mathbf{a}}_k\right]_3}\cdot e^{j\angle\{[\widehat{\mathbf{a}}_k]_4/[\widehat{\mathbf{a}}_k]_3\}} \end{bmatrix} \\ &= \begin{bmatrix} -\cot\theta_k\cos\phi_k + \cot\gamma_k\cos\eta_k\dfrac{\sin\phi_k}{\sin\theta_k} \\ -\cot\theta_k\sin\phi_k - \cot\gamma_k\cos\eta_k\dfrac{\cos\phi_k}{\sin\theta_k} \end{bmatrix} \\ &\quad + j\begin{bmatrix} -\cot\gamma_k\sin\eta_k\dfrac{\sin\phi_k}{\sin\theta_k} \\ \cot\gamma_k\sin\eta_k\dfrac{\cos\phi_k}{\sin\theta_k} \end{bmatrix} \end{aligned} \tag{21}$$

Therefore, the coarse 2D DOA estimates can be derived from the following closed-form formulas [23]:

$$\phi_k^{\text{coarse}} = \begin{cases} \arctan\left\{\dfrac{-\text{Im}\{[\mathbf{q}_k]_1\}}{\text{Im}\{[\mathbf{q}_k]_2\}}\right\}, & \text{Im}\{[\mathbf{q}_k]_2\}\sin\eta_k \geq 0 \\ \arctan\left\{\dfrac{-\text{Im}\{[\mathbf{q}_k]_1\}}{\text{Im}\{[\mathbf{q}_k]_2\}}\right\} + \pi, & \text{Im}\{[\mathbf{q}_k]_2\}\sin\eta_k < 0 \end{cases} \quad (22)$$

$$\theta_k^{\text{coarse}} = \begin{cases} \arctan\left(\dfrac{1}{Q_k}\right), & Q_k \geq 0 \\ \arctan\left(\dfrac{1}{Q_k}\right) + \pi, & Q_k < 0 \end{cases} \quad (23)$$

$$Q_k = -\text{Re}\{[\mathbf{q}_k]_1\}\cos\phi_k^{\text{coarse}} - \text{Re}\{[\mathbf{q}_k]_2\}\sin\phi_k^{\text{coarse}} \quad (24)$$

Moreover, the polarization parameters are also readily to be obtained in the closed-form

$$\eta_k = -\angle\left([\mathbf{q}_k]_1 \sin\phi_k^{\text{coarse}} - [\mathbf{q}_k]_2 \cos\phi_k^{\text{coarse}}\right) \quad (25)$$

$$\gamma_k = \text{arccot}\left(\frac{\text{Im}\{[\mathbf{q}_k]_2 \sin\theta_k^{\text{coarse}}\}}{\cos\phi_k^{\text{coarse}} \sin\eta_k}\right) \quad (26)$$

Accordingly, the coarse direction-cosine estimation for the x and y axes can be calculated, respectively, as follows:

$$\widehat{u}_k^{coarse} = \sin\widehat{\theta}\cos\widehat{\phi} \quad (27)$$

$$\widehat{v}_k^{coarse} = \sin\widehat{\theta}\sin\widehat{\phi} \quad (28)$$

These 2D coarse direction-cosine estimates can then be applied to disambiguate the phase ambiguities in the fine estimates, which are induced from the interdipole and intersubarray spatial displacement.

3.4. Disambiguation Algorithm. Note that when d_x and d_y are much greater than half a wavelength, the estimated values u_k^{fine} and v_k^{fine} in (20) and (17) will be cyclically ambiguous, which is demonstrated as follows:

$$\widehat{u}_k^{fine,n_1} = \widehat{u}_k^{fine} + \frac{\lambda}{d_x} n_1 \quad (29)$$

$$\left\lceil \frac{d_x}{\lambda}\left(-1 - \widehat{u}_k^{fine}\right)\right\rceil \leq n_1 \leq \left\lfloor \frac{d_x}{\lambda}\left(1 - \widehat{u}_k^{fine}\right)\right\rfloor \quad (30)$$

$$\widehat{v}_k^{fine,n_2} = \widehat{v}_k^{fine} + \frac{\lambda}{d_y} n_2 \quad (31)$$

$$\left\lceil \frac{d_y}{\lambda}\left(-1 - \widehat{v}_k^{fine}\right)\right\rceil \leq n_1 \leq \left\lfloor \frac{d_y}{\lambda}\left(1 - \widehat{v}_k^{fine}\right)\right\rfloor \quad (32)$$

Herein, the $\lceil\cdot\rceil$ operator returns the smallest integer greater than its argument, and the $\lfloor\cdot\rfloor$ operator returns the largest integer less than its argument. As such, this process generates a set of cyclically ambiguous estimations.

Then, the coarse 2D DOA estimation results are applied as reference values for choosing a set of highly accurate and unambiguous direction-cosine estimates from the set of ambiguous estimates. This is conducted by first defining the following highly accurate and unambiguous direction-cosines for the x and y axes, respectively. Note that the direction-cosines estimates in [22] require two independent eigendecomposition operations; thus they require additional parameter matching procedure. On the contrary, the direction-cosines estimates in the proposed scheme are obtained from only one eigendecomposition, and therefore, the fine and coarse direction-cosine estimates for the x and y axes are automatically paired without any extra operation.

$$n_{1,\text{opt}} = \arg\min_{n_1}\left\{\left|\widehat{u}_k^{fine,n_1} - \widehat{u}_k^{coarse}\right|\right\} \quad (33)$$

$$n_{2,\text{opt}} = \arg\min_{n_2}\left\{\left|\widehat{v}_k^{fine,n_2} - \widehat{v}_k^{coarse}\right|\right\} \quad (34)$$

These terms are then applied to obtain highly accurate and unambiguous 2D-DOA parameter estimations as follows:

$$\theta_k^{fine} = \arcsin\left(\sqrt{\left(\widehat{u}_k^{fine,n_{1,opt}}\right)^2 + \left(\widehat{v}_k^{fine,n_{2,opt}}\right)^2}\right) \quad (35)$$

$$\phi_k^{fine} = \text{arccot}\left(\frac{\widehat{u}_k^{fine,n_{1,opt}}}{\widehat{v}_k^{fine,n_{2,opt}}}\right) \quad (36)$$

Consequently, the polarization parameter estimations can be updated by substituting θ_k^{fine} and ϕ_k^{fine} into (24) and (25). Note that the DOA and polarization estimates are automatically paired without any extra operation.

3.5. Implementation of the Algorithm. Note that the exact covariance matrices and subspaces are utilized in the previous subsections, but the theoretical covariance matrix like $\mathbf{R}_X$ in (11) is unavailable due to the limited number of L snapshots. In practical, it can be estimated as

$$\widehat{\mathbf{R}}_X = \frac{1}{L}\sum_{t=1}^{L}\left\{\mathbf{x}(t)\,\mathbf{x}^H(t)\right\} \quad (37)$$

Consequently, the procedure of our proposed algorithm is summarized as follows.

Step 1. Estimate the covariance matrix $\mathbf{R}_X$ using (36).

Step 2. Eigendecompose $\mathbf{R}_X$ to generate its signal subspace $\mathbf{E}_s$ as in (13).

Step 3. Partition $\mathbf{E}_s$ into two $4\times K$ matrices $\mathbf{E}_{S1}$ and $\mathbf{E}_{S2}$ via (14) and (15).

Step 4. Eigendecompose $\mathbf{E}_{S1}^{\dagger}\mathbf{E}_{S2}$ to obtain its eigenvalues and eigenvectors.

Step 5. The direction-cosine along the y-axis can be estimated by (17).

Step 6. Estimate the manifold matrix of the left-hand side subarray according to (18).

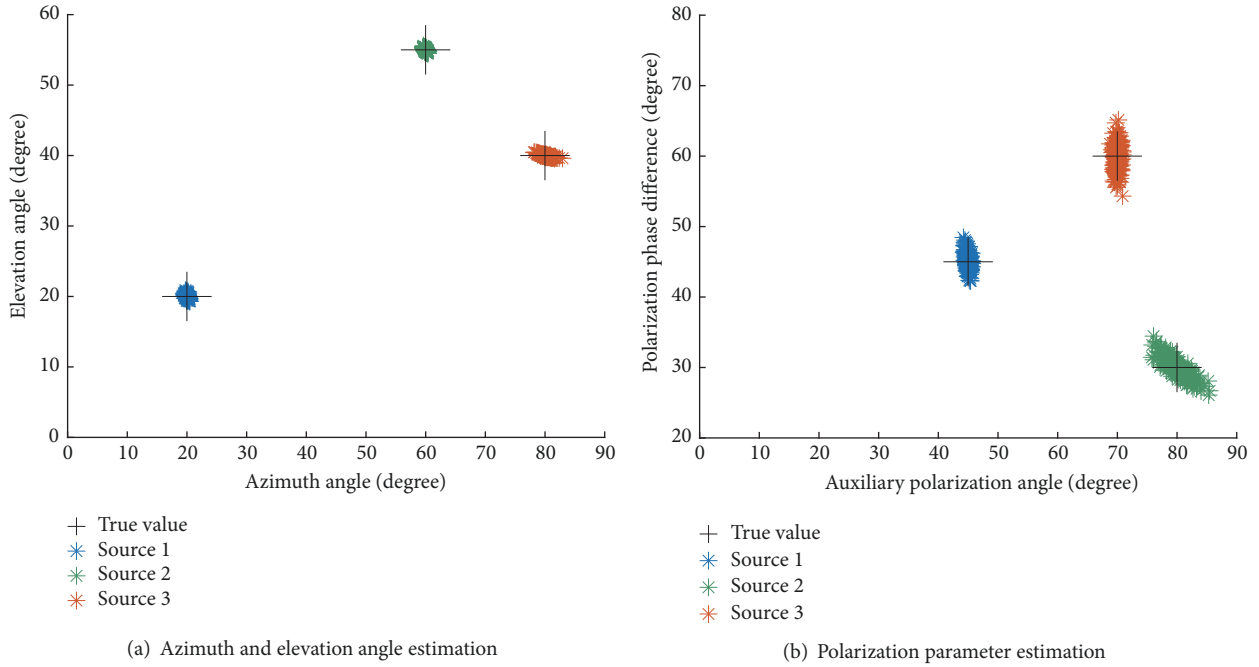

(a) Azimuth and elevation angle estimation

(b) Polarization parameter estimation

FIGURE 2: DOA and polarization estimation results of three sources. The SNR is set equal to 20 dB, the number of snapshots is 100, and 200 independent trials are carried out. (a) Azimuth and elevation angle estimation. (b) Polarization parameter estimation.

Step 7. Obtain the direction-cosines along the x-axis via (20).

Step 8. Construct the 2×1 vector $\mathbf{q}_k$ according to (21), and the coarse DOA estimates can be obtained from (22), (23).

Step 9. The coarse direction-cosine estimates are employed to disambiguate the ambiguities in the fine direction-cosine estimates.

Step 10. The unambiguous direction-cosine estimates are employed for 2D DOA estimation according to (35) and (36), and the polarization parameters are estimated according to (25) and (26).

4. Simulation Results

In this section, several numerical simulations are conducted to validate the performance of the proposed algorithm. The interdipole distance d_x along the x-axis is set as 10λ, and the intersubarray distance d_y along the y-axis is set as 10λ. It is assumed that the number of sources is known *a priori* in the following simulations. And the signal-to-noise ratio (SNR) of the k-th source is defined as $10\log_{10}(\sigma_k^2/\sigma_n^2)$, where σ_n^2 is the noise power and σ_k^2 is the power of the k-th source signal.

In the first experiment, we verify the effectiveness of the proposed algorithm. Consider that there are three uncorrelated equipowered sources impinging on the array. The DOA and polarization parameters are set as $(\theta_1 = 20^\circ, \phi_1 = 20^\circ, \gamma_1 = 45^\circ, \eta_1 = 45^\circ)$, $(\theta_2 = 60^\circ, \phi_2 = 55^\circ, \gamma_2 = 80^\circ, \eta_2 = 30^\circ)$, and $(\theta_3 = 80^\circ, \phi_3 = 40^\circ, \gamma_3 = 70^\circ, \eta_3 = 60^\circ)$, respectively. The number of snapshots is 100 and the SNR equals 20 dB. Figure 2(a) demonstrates the results of the azimuth and elevation angle estimation from 200 independent realizations. Figure 2(b) illustrates the results of the auxiliary polarization angle and polarization phase difference estimation from 200 independent realizations. According to Figure 2, it is evident that the estimated DOA and polarization parameters are correctly paired and almost equal to the true value. Thus, the proposed algorithm can provide high accuracy direction find and polarization estimation results. To further verify the parameter estimation performance versus the SNR and the snapshot number, two more experiments are carried out. The performance is measured in terms of root mean-square error (RMSE) for each individual parameter, which is defined as

$$RMSE = \sqrt{\frac{1}{N}\sum_{n=1}^{N}\left(\hat{y}_{n,k} - y_k\right)^2} \tag{38}$$

where y_k stands for the parameter, $\hat{y}_{n,k}$ denotes the estimation of y_k in the n-th trial, and N is the number of Monte Carlo trials that are conducted in the following simulations, which is 1000.

In the second experiment, the estimation accuracy of the proposed algorithm versus SNR is explored. Consider that two uncorrelated equipowered sources are impinging on the array. DOA and polarization parameters are $(\theta_1 = 30^\circ, \phi_1 = 20^\circ, \gamma_1 = 45^\circ, \eta_1 = -90^\circ)$ and $(\theta_2 = 80^\circ, \phi_2 = 70^\circ, \gamma_2 = 45^\circ, \eta_2 = 90^\circ)$, respectively. The SNR varies from 0 dB to 60 dB in steps of 5 dB. The number of snapshots is fixed at 100. Figure 3 illustrates the RMSEs of DOA and polarization estimation as a function of SNR. Note that, for the azimuth and elevation angle estimates, both the coarse

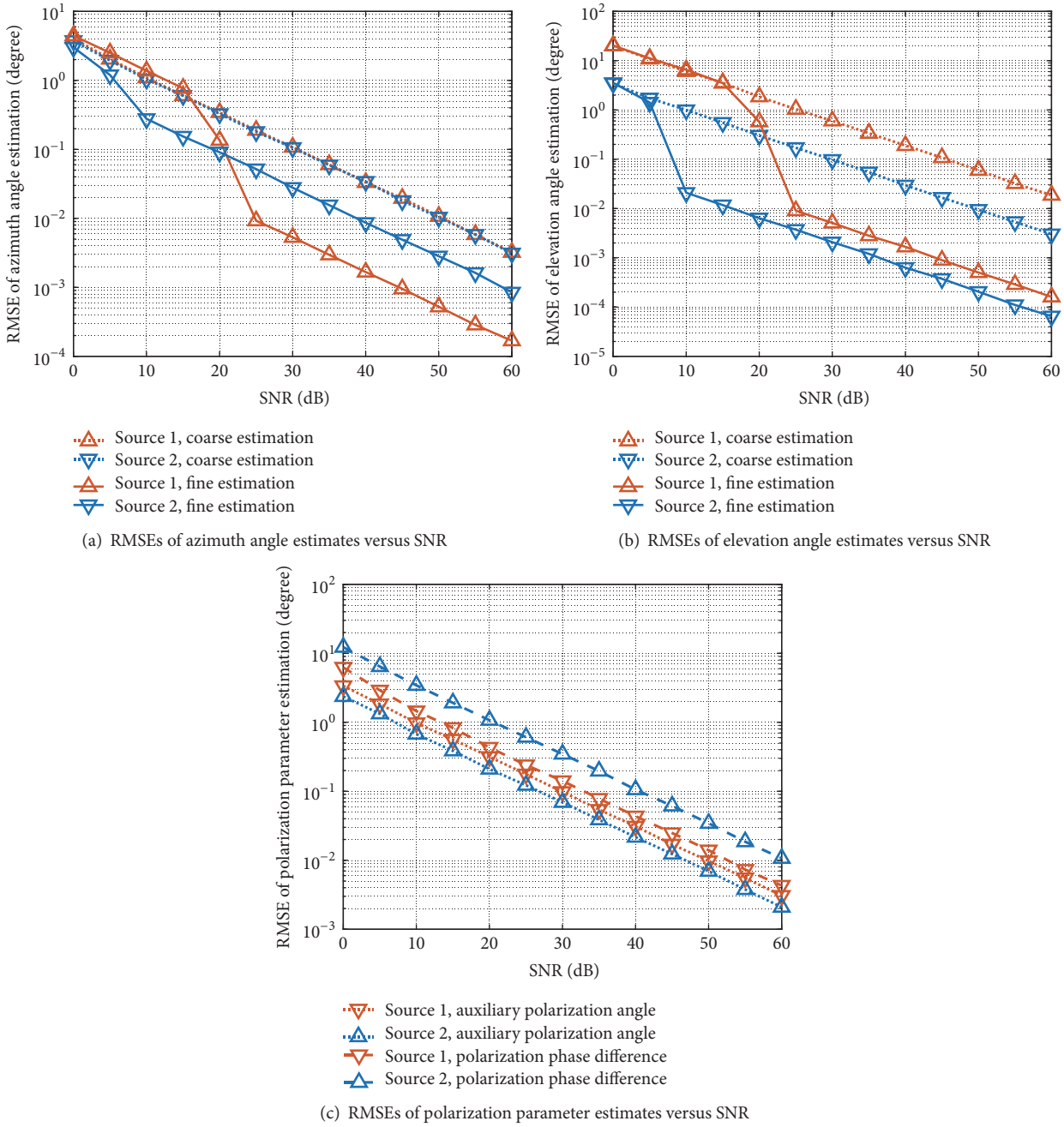

(a) RMSEs of azimuth angle estimates versus SNR

(b) RMSEs of elevation angle estimates versus SNR

(c) RMSEs of polarization parameter estimates versus SNR

Figure 3: RMSEs of DOA and polarization estimation versus SNR for the proposed algorithm. The number of snapshots is 100 and 1000 Monte Carlo trials are carried out. (a) RMSEs of azimuth angle estimates versus SNR; (b) RMSEs of elevation angle estimates versus SNR; (c) RMSEs of the polarization parameter estimation versus SNR.

estimation and the fine estimation results are presented for comparison. From Figures 3(a) and 3(b), it is obvious that the coarse DOA estimates have higher RMSEs since the extended array aperture is not fully utilized. In addition, as is expected, the fine estimates have superior estimation accuracy than the coarse ones after disambiguation. Moreover, the RMSEs of both the DOA and polarization estimates decrease as the SNR increases.

In the third experiment, we investigate the RMSEs of the proposed algorithm with the variation of the number of snapshots. The parameter settings are same as that of the second experiment except that the SNR is set equal to 20 dB, and the number of snapshots varies from 10 to 1000. From Figures 4(a) and 4(b), we can draw a similar conclusion that the fine DOA estimates have superior estimation accuracy than the coarse ones after disambiguation. Moreover, it can

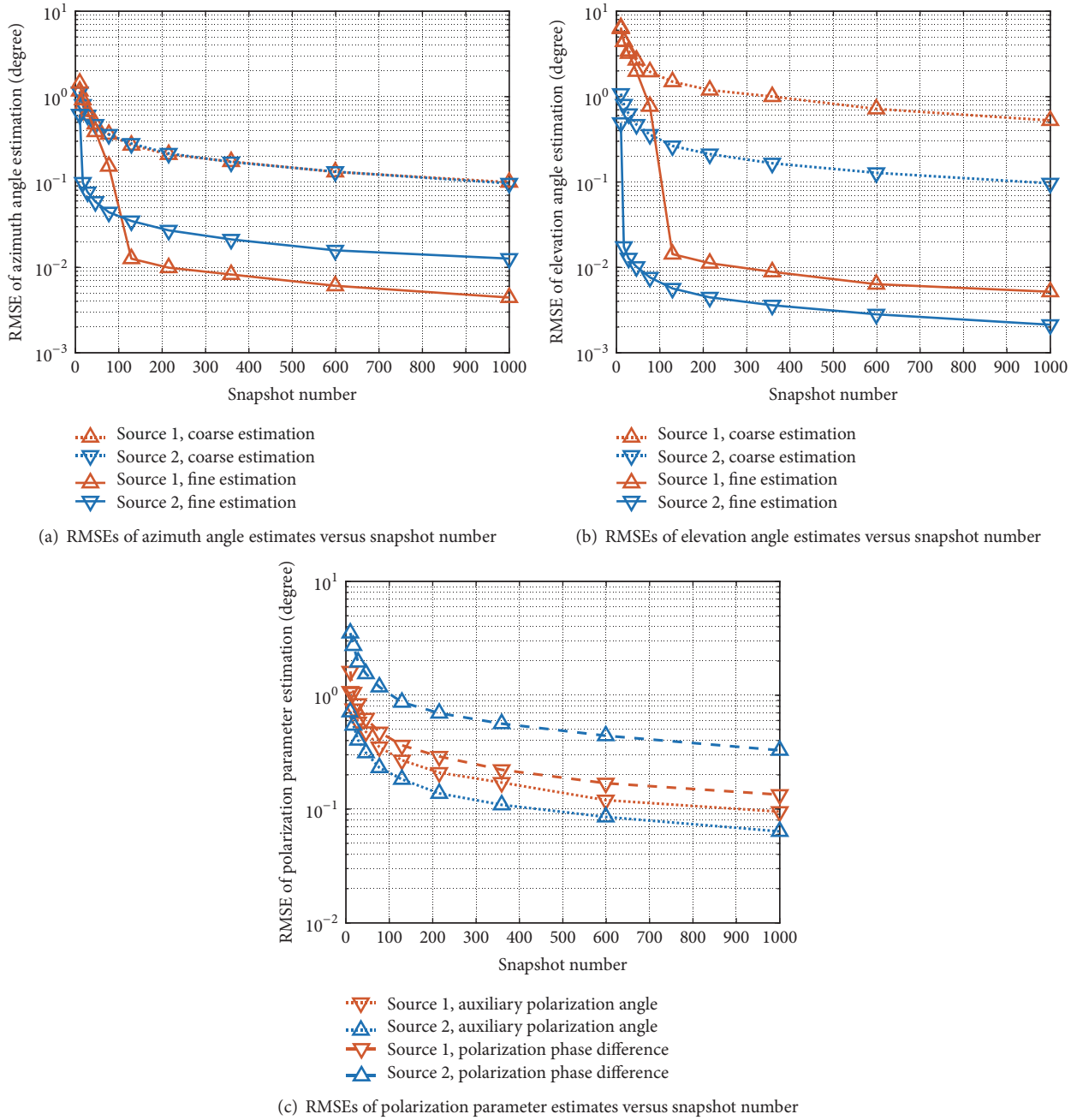

(a) RMSEs of azimuth angle estimates versus snapshot number

(b) RMSEs of elevation angle estimates versus snapshot number

(c) RMSEs of polarization parameter estimates versus snapshot number

Figure 4: RMSEs of DOA and polarization estimation versus snapshot number for the proposed algorithm. The SNR is set equal to 20 dB and 1000 Monte Carlo trials are carried out. (a) RMSEs of azimuth angle estimates versus snapshot number; (b) RMSEs of elevation estimates versus snapshot number; (c) RMSEs of the polarization parameter estimation versus snapshot number.

be observed that the parameter estimation performance of the two sources improves as the snapshot number increases. This is because the fact that a larger sample support will produce better estimate of the covariance matrix for stationary data.

5. Conclusions

This paper developed a joint DOA and polarization estimation algorithm for the proposed two parallel spatially spread dipole arrays. The ESPRIT algorithm is employed for conducting highly accurate and unambiguous coarse parameter estimation based on the spatial rotation invariance of the array structure. The spatially noncollocated array structure is conducive toward reducing the mutual coupling effect and the hardware cost of the electromagnetic vector-sensors array compared with spatially collocated array structures. Moreover, the interelement spacing could be much greater than half a wavelength, which promotes the 2D DOA estimation accuracy.

Data Availability

No data were used to support this study.

Conflicts of Interest

The authors declare no conflicts of interest.

Acknowledgments

This research was funded by the National Natural Science Foundation of China under Grant no. 61601372, Shenzhen Science and Technology Innovation Committee of Basic Research Projects under Grants nos. JCYJ20170306154016149 and JCYJ20170815154325384, China Postdoctoral Science Foundation under Grant no. 2017M613200, Natural Science Basic Research Plan in Shaanxi Province of China under Grant no. 2017JQ6068, and Shanghai Aerospace Science and Technology Innovation Fund under Grant no. sast2017-077.

References

[1] A. Nehorai and E. Paldi, "Vector-sensor array processing for electromagnetic source localization," *IEEE Transactions on Signal Processing*, vol. 42, no. 2, pp. 376–398, 1994.

[2] M. R. Andrews, P. P. Mitra, and R. Decarvalho, "Tripling the capacity of wireless communications using electromagnetic polarization," *Nature*, vol. 409, no. 6818, pp. 316–318, 2001.

[3] R. T. Compton, "The tripole antenna: An adaptive array with full polarization flexibility," *IEEE Transactions on Antennas and Propagation*, vol. 29, no. 6, pp. 944–952, 1981.

[4] C.-Y. Chiu, J.-B. Yan, R. D. Murch, J. X. Yun, and R. G. Vaughan, "Design and implementation of a compact 6-port antenna," *IEEE Antennas and Wireless Propagation Letters*, vol. 8, pp. 767–770, 2009.

[5] N. Le Bihan, S. Miron, and J. I. Mars, "MUSIC algorithm for vector-sensors array using biquaternions," *IEEE Transactions on Signal Processing*, vol. 55, no. 9, pp. 4523–4533, 2007.

[6] A. Nehorai and P. Tichavsky, "Cross-product algorithms for source tracking using an im vector sensor," *IEEE Transactions on Signal Processing*, vol. 47, no. 10, pp. 2863–2867, 1999.

[7] P. Tichavský, K. T. Wong, and M. D. Zoltowski, "Near-field/far-field azimuth and elevation angle estimation using a single vector hydrophone," *IEEE Transactions on Signal Processing*, vol. 49, no. 11, pp. 2498–2510, 2001.

[8] X. F. Gong, Z. W. Liu, and Y. G. Xu, "Quad-quaternion MUSIC for DOA estimation using electromagnetic vector sensors," *EURASIP Journal on Advances in Signal Processing*, vol. 2008, Article ID 213293, pp. 1–14, 2009.

[9] G. Zheng and B. Wu, "Polarisation smoothing for coherent source direction finding with multiple-input and multiple-output electromagnetic vector sensor array," *IET Signal Processing*, vol. 10, no. 8, pp. 873–879, 2016.

[10] K. T. Wong and M. D. Zoltowski, "Uni-vector-sensor ESPRIT for multisource azimuthelevation, and polarization estimation," *IEEE Transactions on Antennas and Propagation*, vol. 45, no. 10, pp. 1467–1474, 1997.

[11] R. Roy and T. Kailath, "ESPRIT-estimation of signal parameters via rotational invariance techniques," *IEEE Transactions on Signal Processing*, vol. 37, no. 7, pp. 984–995, 1989.

[12] M. D. Zoltowski and K. T. Wong, "ESPRIT-based 2-D direction finding with a sparse uniform array of electromagnetic vector sensors," *IEEE Transactions on Signal Processing*, vol. 48, no. 8, pp. 2195–2204, 2000.

[13] G. M. Zheng, "A novel spatially spread electromagnetic vector sensor for high-accuracy 2-D DOA estimation," *Multidimensional Systems and Signal Processing*, vol. 28, pp. 23–48, 2017.

[14] K. T. Wong and M. D. Zoltowski, "Closed-form direction finding and polarization estimation with arbitrarily spaced electromagnetic vector-sensors at unknown locations," *IEEE Transactions on Antennas and Propagation*, vol. 48, no. 5, pp. 671–681, 2000.

[15] K. T. Wong, "Blind beamforming geolocation for wideband-FFHs with unknown hop-sequences," *IEEE Transactions on Aerospace and Electronic Systems*, vol. 37, no. 1, pp. 65–76, 2001.

[16] K. T. Wong, "Direction finding/polarization estimation-dipole and/or loop triad(s)," *IEEE Transactions on Aerospace and Electronic Systems*, vol. 37, no. 2, pp. 679–684, 2001.

[17] D. M. Kitavi, K. T. Wong, M. Zou, and K. Agrawal, "A lower bound of the estimation error of an emitter's direction-of-arrival / polarization, for a collocated triad of orthogonal dipoles/loops that fail randomly," *IET Microwaves, Antennas & Propagation*, vol. 11, no. 7, pp. 961–970, 2017.

[18] S. Khan, K. T. Wong, Y. Song, and W.-Y. Tam, "Large circular loops in the estimation of an incident emitter's direction-of-arrival or polarization," *IEEE Transactions on Antennas and Propagation*, vol. 66, no. 6, pp. 3046–3055, 2018.

[19] K. T. Wong, Y. Song, C. J. Fulton, S. Khan, and W.-Y. Tam, "Electrically 'long' Dipoles in a Collocated/Orthogonal Triad - For Direction Finding and Polarization Estimation," *IEEE Transactions on Antennas and Propagation*, vol. 65, no. 11, pp. 6057–6067, 2017.

[20] K. T. Wong and X. Yuan, "'Vector cross-product direction-finding' with an electromagnetic vector-sensor of six orthogonally oriented but spatially noncollocating dipoles/loops," *IEEE Transactions on Signal Processing*, vol. 59, no. 1, pp. 160–171, 2011.

[21] Y. Song, X. Yuan, and K. T. Wong, "'Errata to' 'Vector cross-product direction-finding' with an electromagnetic vector-sensor of six orthogonally oriented but spatially non-collocating dipoles / loops," *IEEE Transactions on Signal Processing*, vol. 62, no. 4, pp. 1028–1030, 2014.

[22] X. Yuan, "Joint DOA and Polarization Estimation with Sparsely Distributed and Spatially Non-Collocating Dipole/Loop Triads," *Statistics*, 2013.

[23] X. Yuan, "Spatially spread dipole/loop quads/quints: for direction finding and polarization estimation," *IEEE Antennas and Wireless Propagation Letters*, vol. 12, no. 12, pp. 1081–1084, 2013.

[24] X. Gong, J. Jiang, H. Li, Y. Xu, and Z. Liu, "Spatially spread dipole/loop quint for vector-cross-product-based direction finding and polarisation estimation," *IET Signal Processing*, vol. 12, no. 5, pp. 636–642, 2018.

[25] M. Yang, J. Ding, B. Chen, and X. Yuan, "A multiscale sparse array of spatially spread electromagnetic-vector-sensors for direction finding and polarization estimation," *IEEE Access*, vol. 6, pp. 9807–9818, 2018.

[26] B. Li, W. Bai, Q. Zhang, G. Zheng, J. Bai, and X. Fu, "High Accuracy and Unambiguous 2D-DOA Estimation With an Uniform Planar Array of 'Long' Electric-Dipoles," *IEEE Access*, vol. 6, pp. 40559–40568, 2018.

[27] G. Zheng, B. Wu, Y. Ma, and B. Chen, "Direction of arrival estimation with a sparse uniform array of orthogonally oriented and spatially separated dipole-triads," *IET Radar, Sonar & Navigation*, vol. 8, pp. 885–894, 2014.